NJC

Accepted Manuscript

This is an *Accepted Manuscript*, which has been through the Royal Society of Chemistry peer review process and has been accepted for publication.

Accepted Manuscripts are published online shortly after acceptance, before technical editing, formatting and proof reading. Using this free service, authors can make their results available to the community, in citable form, before we publish the edited article. We will replace this *Accepted Manuscript* with the edited and formatted *Advance Article* as soon as it is available.

You can find more information about *Accepted Manuscripts* in the Information for Authors.

Please note that technical editing may introduce minor changes to the text and/or graphics, which may alter content. The journal's standard Terms & Conditions and the Ethical guidelines still apply. In no event shall the Royal Society of Chemistry be held responsible for any errors or omissions in this *Accepted Manuscript* or any consequences arising from the use of any information it contains.

ROYAL SOCIETY OF CHEMISTRY

www.rsc.org/njc

Graphic Abstract

High-yield synthesis of poly(m-phenylenediamine) hollow nanostructures by diethanolamine-assisted method and their enhanced ability for Ag^+ adsorption

Zhen Su[a,c], Liyuan Zhang[a,c], Liyuan Chai[a,b], Haiying Wang[*a,b], Wanting Yu[a], Ting Wang[a], Jianxiong Yang[a]

[a]Department of Environmental Engineering, School of Metallurgy and Environment, Central South University, Changsha 410017, China; [b]National Engineering Research Center for Heavy Metals Pollution Control and Treatment, Changsha 410017, China

DEA induces the formation of PmPD hollow nanostructures which exhibit improved adsorption performance.

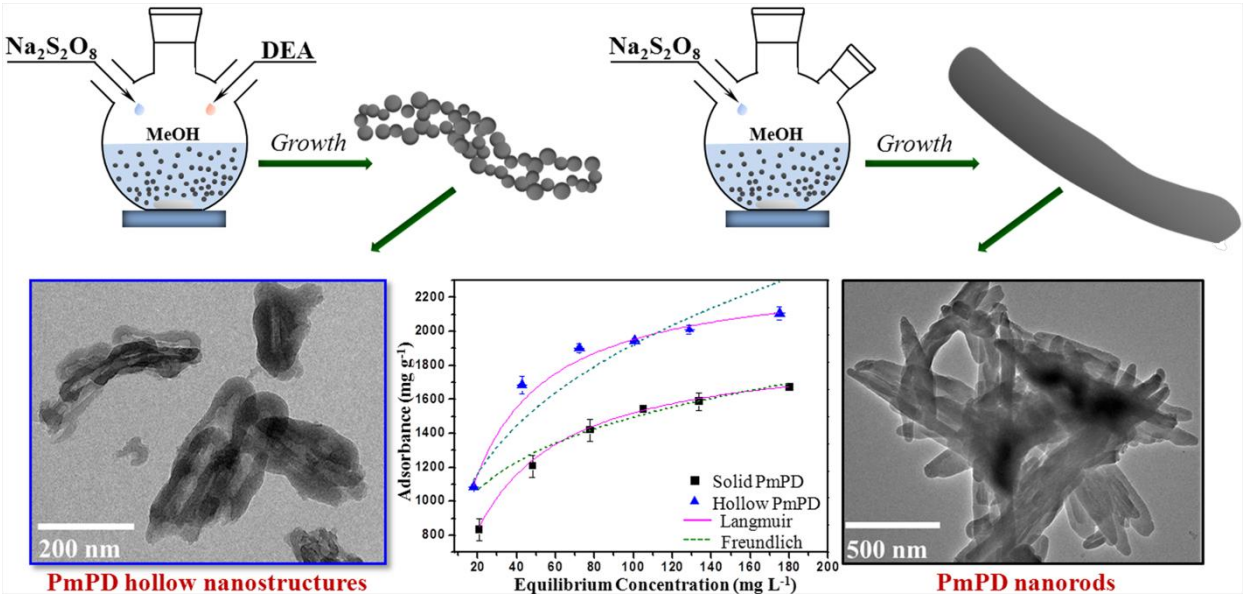

* Corresponding author: Tel.: +86-0731-88836804; fax: +86-0731-88710171. E-mail address: haiyw25@yahoo.com (H.W).

Cite this: DOI: 10.1039/c0xx00000x

www.rsc.org/xxxxxx

ARTICLE TYPE

High-yield synthesis of poly(m-phenylenediamine) hollow nanostructures by diethanolamine-assisted method and their enhanced ability for Ag^+ adsorption

Zhen Su[a,c], Liyuan Zhang[a,c], Liyuan Chai[a,b], Haiying Wang*[a,b], Wanting Yu[a], Ting Wang[a], Jianxiong Yang[a]

Received (in XXX, XXX) Xth XXXXXXXXX 20XX, Accepted Xth XXXXXXXXX 20XX
DOI: 10.1039/b000000x

A diethanolamine-assisted (DEA-assisted) method was explored to synthesize the hollow nanostructures of poly(m-phenylenediamine) (PmPD) with high specific surface area through conventional oxidation method. DEA concentration has a significant influence on the PmPD morphology and the possible formation mechanism has been proposed. The obtained hollow nanostructures show excellent Ag^+ adsorption ability with the adsorbance of 2359.3 $mg \cdot g^{-1}$, much higher than other reported materials.

Introduction

Poly(phenylenediamine)s (PPDs), diamine derivative of polyaniline, have received much attention due to its multifunctionality and application prospect in various fields.[1-4] Particularly, the adsorption characteristic of PPDs has been widely reported over the past decade because of their powerful redox reversibility and chelation ability.[5, 6] Among the PPDs, poly(m-phenylenediamine) (PmPD) is generally considered as a more effective adsorbent for its simple preparation and extremely high solvent resistance. Poly(p-phenylenediamine) with linear or ladder structures tend to be soluble in most common solvents and poly(o-phenylenediamine) usually need a high temperature (above 100 ˚C) to initiate the polymerization. Till now, many research groups including ours have demonstrated the distinguished adsorption performance of PmPD towards Ag^+, Pb^{2+}, Hg^{2+}, Cr^{6+}, SO_4^{2-} and organic dye, *etc*.[3, 7-13]

Morphology-dependent application has become the research focus in recent years. Especially, materials with hollow structures are promising in many fields because of their low density, interesting structure and high surface area.[14-16] At present, hollow nanostructures of polyaniline and poly(o-/p-phenylenediamine) have been successfully fabricated and offered fantastic applications .[16-21] As for PmPD, most of them are micron-sized or solid despite the fact that various morphologies have been synthesized.[7, 22-24] In addition, the general chemical methods to prepare hollow structures often involve with the usage of soft/hard templates, surfactants or metal ions, which will lead to either complex preparation process or undesired introduction of impurity on products. Therefore, it is meaningful to develop a facile method to synthesize PmPD hollow nanostructures in order to promote its application performance.

In present research, we successfully prepared the PmPD hollow nanotubes with rough surface, for the first time, by a template-less polymerization route with the assistance of DEA through conventional chemical oxidation. This method is simple and the obtained product is pure, high-yield and in a relatively low oxidation state. What's more, the Ag^+ adsorption ability of the resulting hollow nanostructures is superior.

Experimental

Chemicals

Sodium persulfate, m-phenylenediamine (mPD), methanol, diethanolamine (DEA), dipropylamine (DPA), tetrahydrofuran (THF), ethanol (EtOH), N-methyl-2-pyrrolindone (NMP), ammonia-water, and silver nitrate ($AgNO_3$) were of analytical grade.

Preparation of Poly(m-phenylenediamine)

The typical procedure for the synthesis is as follows: 3.0 g of mPD was added to 100 mL of methanol solution in a 250 mL of five-necked round-bottom flask with magnetic stirring at 30 ˚C for 15 min. 6.6 g of sodium persulfate (oxidant/monomer molar ratio is 1) was dissolved in 20 mL of distilled water as an oxidant solution. The polymerization was initiated by using syringe pump to gradually add oxidant solution at a rate of 2 $mL \cdot min^{-1}$. Synchronously, 20 mL of DEA methanol solution of certain concentration was added dropwise into the reaction system. Then the reaction mixture was stirred for another 3 h at 30 ˚C. The final products were collected by filtration, rinsed with distilled water, ammonia-water, and absolute ethanol respectively. Finally, the product was dried at 60 ˚C in air for 12 h. The yield of the product was calculated by the equation (1):

$$Y = \frac{m}{M} \times 100\% \quad (1)$$

where Y represents the yield (%), m is the mass (g) of the product; M is the mass (g) of the monomer. The sample prepared without

adding DEA was named as PmPD-NM and other samples were denoted as PmPD-DEA***x*** (***x***=0.5, 1, 2.0), according to the concentration of DEA introduced.

Adsorption Experiments

During the whole adsorption experiments, Ag^+ solutions were kept in the dark circumstance. The investigation for the kinetic adsorption behavior of PmPD was conducted. 25 mg of PmPD was added into 20 mL of $AgNO_3$ aqueous solution with an initial concentration of 46 mM at 30 °C for a specific time (0-82 h). The initial pH of the solution was controlled by HNO_3 or NaOH. After a desired treatment period, the solution was then withdrawn and filtered through quantitative filter paper. The Ag^+ concentration in the filtrate was detected by the Volhard titration method. All experiments were replicated thrice and results were averaged. The Ag^+ adsorbance of PmPD-NM and PmPD-DEA***x*** was calculated by equation (2). The kinetic process of adsorption was tested by pseudo-first (3) and -second (4) equations,

$$Q = \frac{(C_0 - C_1)}{M} \times V \quad (2)$$

$$Q_t = Q_e(1\text{-}e^{-kt}) \quad (3)$$

$$Q_t = \frac{hQ_e^{\,2}t}{1 + hQ_e t} \quad (4)$$

where Q (mg·g^{-1}) is the Ag^+ adsorbance of PmPD, C_0 is the initial concentration of Ag^+ and C_1 is the final concentration of Ag^+. M (mg) is the dosage of PmPD and V (mL) is the volume of Ag^+ solution, Q_e (mg·g^{-1}) are the equilibrium Ag^+ adsorbance of the PmPD, Q_t is the adsorbance of the PmPD at certain time (t, h), k and h are the rate constants of first and second order equations, respectively.

The isotherm adsorption manipulation was similar to that of kinetics but the adsorption time was fixed at 72 h. Langmuir (5) and Freundlich (6) models were used to study the isotherm adsorption behavior of the PmPD-NM and PmPD-DEA***x***,

$$Q_e = \frac{Q_m K_a C_e}{1 + K_a C_e} \quad (5)$$

$$Q_e = K_f C_e^{\,1/n} \quad (6)$$

where Q_m (mg·g^{-1}) represents the maximum adsorption capability, C_e (mg·L^{-1}) is the equilibrium concentration of Ag^+, K_a (L·mg^{-1}) is the adsorption coefficient, K_f and n are the equilibrium constants.

Competitive adsorption was carried out with the identical conditions as above besides introducing coexisting metal ions. The initial concentration of the metal ions is 10 mM. The concentration of metal ions was measured with inductively coupled plasma.

Characterization

Scanning electron microscope (SEM JSM6360) and transmission electron microscope (TEM TECNAI G^2) were used to investigate the size and morphology of PmPD. FTIR spectra was conducted on a pressed pellet with KBr using Nicolet IS10 infrared spectrometer at 4 cm^{-1} resolution. The BET method was used to calculate the surface area of PmPD. The pore volume was calculated from the adsorption branches of the isotherm by BJH method. Thermal stability of the product was tested by the SETSYS Evolution thermo analyser under air atmosphere at a heating rate of 20 °C min^{-1}. The X-ray diffraction (XRD) pattern was collected on a D/Max 2500 VB+X X-ray diffractometer using Cu (40 kV, 300 mA) radiation.

The solubility was investigated semiquantitatively as follows: 10 mg of sample was added into 10 ml of the specific solvent and the solution was shaken for 24 h at room temperature. Then the solution was filtered to acquire the filtrate for calculation.[25] In this study, all products are insoluble or slightly soluble in the organic solvents.

Results and Discussion

Generally, conventional chemical oxidative method that features dropwise adding the oxidant into the monomer solution has the virtue of high yield and good operating security. However, due to secondary growth, it is difficult to obtain the nano-sized particles, let alone the nanoparticles with hollow architecture. Although our group has successfully synthesized PmPD nanorods by conventional polymerization through changing the solvent to methanol, this method is still not capable of preparing its hollow nanostructures. In this system, based on the conventional polymerization using methanol as solvent, DEA was synchronously added when dropping oxidant into the monomer solution to successfully produce hollow nanostructures of PmPD.

Morphology and yield of PmPD

Fig. 1 gives the typical SEM and TEM images of the PmPD synthesized with and without adding the DEA during the polymerization process. As seen in Fig. 1A and 1B, without DEA, the resulting product (PmPD-NM) is mainly composed of nanorods with the diameter of ~100 nm and the length of 130~500 nm. The specific surface area is 32.6 m^2·g^{-1} and pore volume is 0.041 cm^3·g^{-1} as measured by BET method and BJH method respectively (Table 1). However, when synchronously adding DEA (~1.0 M) into the reaction system, the size of the obtained sample (PmPD-DEA***1***) becomes smaller with the average diameter of ~75 nm and length of 150~320 nm (Fig. 1C), confirmed by the TEM images (Fig. 1D). More importantly, the one-dimensional (1D) nanostructures are hollow with the wall thickness ranging from 15 nm to 35 nm. The surface of the nanotubes is not smooth, showing asperities along the tubes. Its surface area (60.2 m^2·g^{-1}) and pore volume (0.254 cm^3·g^{-1}) dramatically increases by about 2 times and 6 times respectively than those of PmPD-NM. Obviously, the participation of DEA is conductive to the formation of hollow morphology of PmPD, which can further promote its adsorption application.

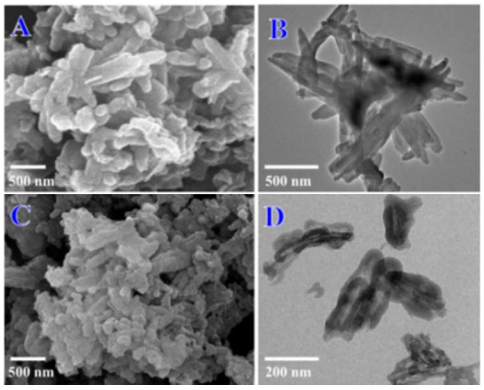

Fig. 1 SEM (left) and TEM (right) images of PmPD synthesized by chemical oxidative polymerization. (A, B): without adding DEA; (C, D) adding DEA (~1.0 M) solution.

Moreover we examined the effect of DEA concentration on the morphology of PmPD. When the DEA concentration is 0.5 M, the morphology and size of the product (PmPD-DEA***0.5***) are similar to PmPD-NM, but its surface become a little rough. Moreover, the specific surface area (38.5 $m^2 \cdot g^{-1}$) and pore volume (0.113 $cm^3 \cdot g^{-1}$) are higher than PmPD-NM (Fig. 2A and 2B). When increasing the DEA concentration to ~2.0 M, the size of PmPD-DEA***2.0*** become much larger than other samples with the diameter of ~500 nm and average length of ~1.5μm (Fig. 2C and 2D). Furthermore, as compared to PmPD-DEA***1.0***, the surface area (38.6 $m^2 \cdot g^{-1}$) and pore volume (0.179 $cm^3 \cdot g^{-1}$) of PmPD-DEA***2.0*** sharply decline. This indicates that high DEA concentration is disadvantageous to the enhancement of surface area. Based on the above analysis, it can be concluded that appropriate concentration of DEA is critical to maximize the surface area and pore volume of PmPD. Herein, ~1.0 M of DEA is an optimal choice.

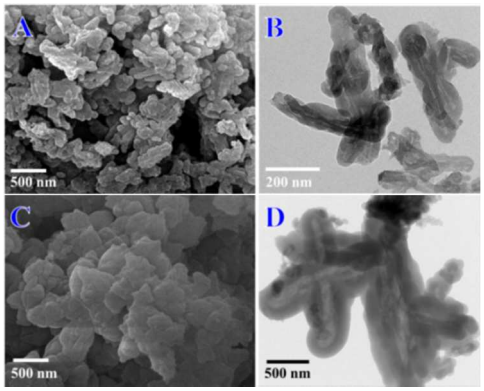

Fig. 2 SEM and TEM images of PmPD synthesized with the DEA concentration of 0.5 M (A, B); 2 M (C, D).

Besides the morphology, yield is another essential parameter. By increasing the DEA concentration, the variation trend of yield first increases and then descends (Table 1). PmPD-DEA***1.0*** owns the highest yield (87.5 %), nearly 17 % larger than that of PmPD-NM. This demonstrates that DEA could promote the reactivity of monomer and thus boost the yield. However, high DEA content tends to weaken oxidizability of persulfate oxidant which would in-turn restrict the polymerization. That's why the yield drops when further increasing DEA concentration. When the DEA concentration increases to ~5.0 M, the yield falls to only 68.1 %.

Combing the above discussion, large-scale synthesis of PmPD hollow nanostructures with high surface area and pore volume can be successfully prepared by the DEA-assisted method when using methanol as solvent, which can hardly be accomplished through current chemical methods. These properties will render the product a bright prospect for the adsorption performance.

Characterizations of PmPD

The molecular structure of the PmPD was studied with FTIR (Fig. 3). The PmPD prepared under different DEA concentration has similar IR adsorption. The broad peaks between 3500-3000 cm^{-1} correspond to the stretching vibration of -NH- groups.[26] The two peaks at 1620 cm^{-1} and 1500 cm^{-1} are owing to the stretching mode of quinoid imine and benzenoid amine units, respectively. The adsorption bands at 1250 cm^{-1} are attributed to the C-N stretching vibration in the benzenoid amine units.[27-29] The peak at 1044 cm^{-1} suggests the presence of sulfonated groups covalently attached to the aromatic rings.[30] It should be noticed that by increasing the DEA concentration the intensity of benzenoid amine stretching mode (1500 cm^{-1}) increases as comparing to that of quinoid imine (1620 cm^{-1}). That is to say DEA is in favor of lowering the oxidation state of PmPD. The low oxidation state of PmPD can potentially promote the application prospect for removing metal ions from water.[5]

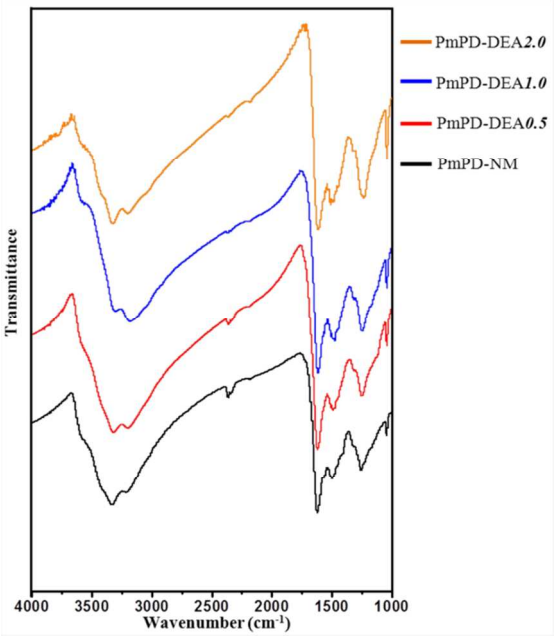

Fig. 3 FTIR spectra of PmPD-NM and PmPD-DEA***x*** (***x=0.5***, ***1.0***, ***1.5***, ***2.5***).

XRD was performed to investigate the macromolecular arrangement of PmPD, which plays an important role in adsorption application. The five samples present a broad diffraction peak between 20° and 23° (Fig. S1), a typical diffraction of amorphous structure.[9] And the large intermolecular spacing and amorphousness are commonly believed to favour the adsorption application of PmPD-DEA***x*** (***x=0.5***, ***1.0***, ***2.0***).

In addition, the solubility of PmPD in H_2O, THF, EtOH and NMP is shown in Table 1. As seen, the solubility of the six samples in H_2O, THF, EtOH and NMP is very poor, which is insoluble or slightly soluble. In addition, the TG characterization conducted in air condition indicates that all the samples own good

thermal stability and the full degradation temperature are above 745 °C (Fig. S2), much higher than that of the polyaniline.[31]

Table 1 Yield, pore volume, specific surface area, degradation temperature and solubility of PmPD prepared with different DEA concentrations.

PmPD -name	Yield (%)	Pore volume ($cm^3 \cdot g^{-1}$)	Specific surface area ($m^2 \cdot g^{-1}$)	Solubility[a]			
				H_2O	THF	EtOH	NMP
NM	70.6±1.1	0.041	32.6	IS	IS	IS	SS
DEA***0.5***	80.2±1.3	0.113	38.5	IS	SS	SS	SS
DEA***1.0***	87.5±2.0	0.254	60.2	IS	SS	SS	SS
DEA***2.0***	85.1±1.5	0.179	38.6	IS	SS	SS	SS

[a] IS and SS represent the sample is insoluble or slightly soluble in a specific solvent.

DEA function on the polymerization

It is well-known that during the oxidative polymerization of aromatic amine, abundant H^+ will be released, which can protonate monomers, oligomer and polymer to further abate their reactivity.[5, 32] However, the introduction of DEA, one kind of hydramine, can balance the acidity of the system and exert significant influences on the polymerization process.

To understand the function of DEA on the morphology of PmPD, several samples were separated when adding 10 wt%, 30 wt% and 70 wt% of oxidant and characterized with TEM.

The polymerization in methanol system without adding DEA has been investigated in our previous study.[7] During the morphology evolution, nanospheres (20~55 nm, Fig. 4A) formed at the initial stage have strong tendency to aggregate to the rod-like morphology (30 wt%, Fig. 4B) and then grow into integrated fibres (70 wt%, Fig. 4C) with the average diameter of ~110 nm. When introducing DEA into the reaction system, however, the PmPD nanoparticles (15~20 nm, Fig. 4D) formed initially tend to gather in a loose manner (30 wt%, Fig. 4E), which is different from that without using DEA (Fig. 4B). Furthermore, the sample obtained after adding 70 wt% of oxidant becomes interesting 1D hollow structures with rough surface (60~100 nm in diameter, Fig. 4F).

Moreover, apart from the above TEM observation, a comparative experiment was designed by using DPA [$(CH_2)_3NH(CH_2)_3$] instead of DEA [$OH(CH_2)_2NH(CH_2)_2OH$] to assist the polymerization of mPD. The only difference between these two organic amines is that the hydroxyl groups on DEA are substituted by alkyl groups on DPA. As a result, the final product is solid and the analogous hollow structures cannot be found (Fig. S3). That means hydroxyl groups on DEA play an indispensable role in mediating the loose assembly of the initially-formed nanoparticles.

Based on the above information, a possible explanation is given to elucidate the morphology evolution of PmPD synthesized by DEA-assisted method. As adding DEA into the reaction system, the protonation extent of the monomer and polymer will be restrained because DEA can neutralize the generated H^+. Thus abundant amino groups on the PmPD chains are non-protonated and this fact is supposed to be an important prerequisite to a further interaction between DEA and PmPD nanoparticles. It is reasonable that the non-protonated amino groups that have lone pairs of electrons on polymer chains is assumed to form hydrogen bonds with the hydroxyl groups on DEA molecules,[33, 34] thereby making DEA clung tightly to PmPD particles. It should be noted that DEA is highly soluble in methanol. As a consequence, the DEA-attached nanoparticles are more inclined to be dispersive in methanol as comparing to the DEA-free system. In other words, the aggregation trend might be lessened in the presence of DEA, leading to the loose piling of the pre-formed nanoparticles and finally the appearance of hollow morphology. On the other hand, a high DEA concentration leads to large-size PmPD tubes, (e.g., PmPD-DEA***2.0***). The reason for the large size may be attributed to the improved intermolecular interaction between DEA and PmPD, since increased amounts of released H^+ ions are neutralized under high DEA concentration. Then this strengthened interaction force can better prevent the aggregation tendency of the pre-formed particles, meaning the nanoparticles will have more time to grow bigger before integrating. Thereby, enlarged hollow micromorphology with low surface area is produced. The possible formation process is illustrated in Scheme 1.

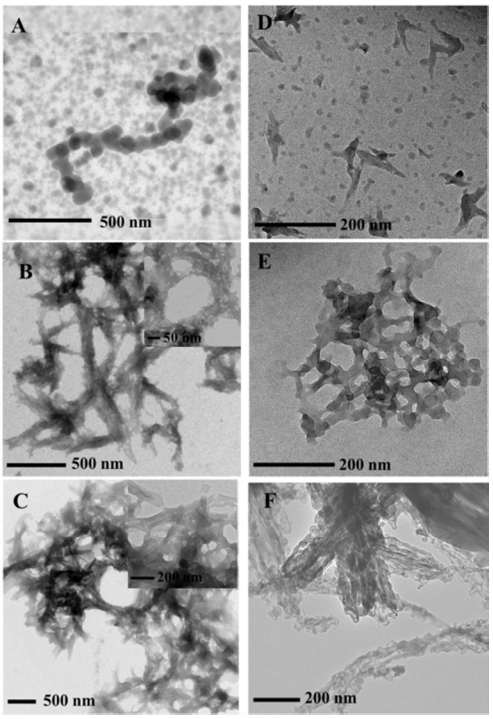

Fig. 4 TEM images of products separated after adding A: 10 wt%, B: 30 wt%, C: 70 wt% of oxidant without DEA and D: 10 wt%, E: 30 wt%, F: 70 wt% with the aid of ~1.0M DEA.

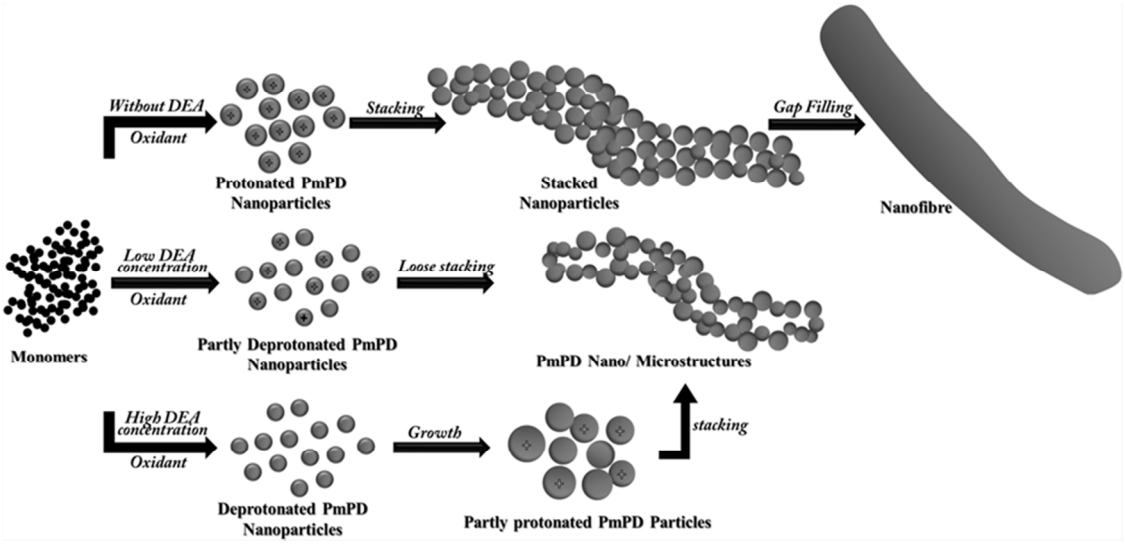

Scheme 1. A possible growth route of PmPD prepared with or without the addition of DEA.

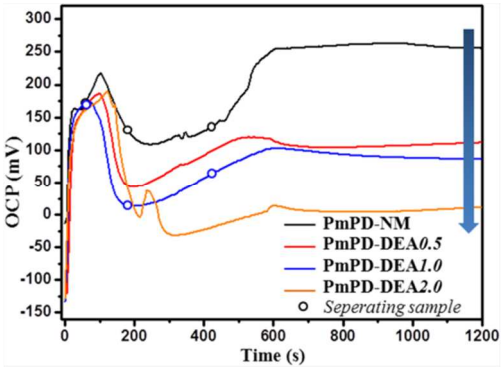

Fig. 5 Open-circuit potential measured during the polymerization.

Additionally, to see the influence of DEA on polymerization, open-circuit potential (OCP) was measured and shown in Fig. 4. The OCP curves first rise sharply due to the sudden addition of oxidant and then decrease rapidly to a minimum value, meaning the formation of oligomer. After that, the OCP increases again slowly until the oxidant solution added up, which corresponds to the chain propagation.[35] And it can be seen that the final polymerization potential gradually decreases as increasing the DEA concentration, indicating the lowering oxidation state of the final particles.[5] This conclusion is consistent with the FTIR result and the phenomenon is due to the restraint of the release of H^+ produced during the polymerization through adding alkali.[5] Besides, due to the neutralization of protons by DEA, the reactivity of the monomer, oligomer and polymer increases, thus promoting the yield of PmPD.

Ag^+ adsorption ability of PmPD

Effect of initial pH. Ag^+ adsorption of PmPD-NM was measured with initial pH value from 1.8 to 6.0 (Fig. 6). The adsorptivity was calculated according to the equations described in the literature.[36] When decreasing the pH from 4.0 to 1.8, the adsorptivity declines obviously from only 22.8 % to 11 %. This means that the acidic condition is not beneficial for Ag^+ removal. While at pH 4.0~6.0, the adsorptivity varies little (< 2 %), suggesting the weak acidic condition influences slightly on Ag^+ adsorption. As a consequence, the solution pH at 5.0~6.0 is more suitable for Ag^+ adsorption.

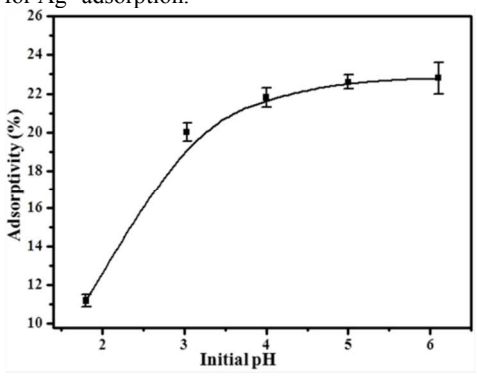

Fig. 6 Effect of initial pH on Ag^+ adsorption with PmPD-NM. Initial concentration of Ag^+ is 60 mM.

Effect of initial Ag^+ concentration. Fig. 7(a) gives the Ag^+ adsorption performances of PmPD versus Ag^+ concentration (0~200 mM). For PmPD-NM, the adsorbance rapidly reaches to 1420 $mg \cdot g^{-1}$ when the initial concentration goes up to 94 mM. Then the enhancement of the adsorbance gradually decreases as further increasing the Ag^+ concentration. Finally, the adsorbance of PmPD-NM reaches to 1672 $mg \cdot g^{-1}$ with the initial Ag^+ concentration of 200 mM. As for PmPD synthesized with the DEA-assisted method, the adsorbance is obviously higher than PmPD-NM. Noticeably, the adsorbance of PmPD-DEA***1.0*** achieves the highest value (2107 $mg \cdot g^{-1}$) with the initial Ag^+ concentration of 200 mM. However, the Ag^+ adsorbance declines when using PmPD-DEA***2.0*** as adsorbent, which may be ascribed to its decreased surface area and pore volume.

Langmuir and Freundlich math models are used to analyse the adsorption equilibrium of Ag^+ onto the PmPD. The isotherms based on the experimental data and the parameters obtained from nonlinear regression by both models are shown in Fig. 7(b). Table 2 summarizes the determination coefficients (R^2) of the Langmuir and Freundlich isotherms of different samples. It appears that the Langmuir can better describe the adsorption behavior since it has a higher R^2 (>0.99). On basis of the Langmuir model, the theoretical Ag^+ adsorption capacities are 1920.8 $mg \cdot g^{-1}$ for PmPD-NM, 2016.9 $mg \cdot g^{-1}$ for PmPD-DEA***0.5***, 2359.3 $mg \cdot g^{-1}$ for

PmPD-DEA***1.0***, and 2132.5 mg·g^{-1} for PmPD-DE***2.0***.

The adsorption performances of some other materials have been listed in Table S1 for comparison. The conducting polyaniline and its derivatives or copolymer possess more powerful adsorbability for Ag^+ (530~2050 mg·g^{-1}) while other common adsorbents, such as modified vermiculite (69 mg·g^{-1}) and activated carbon (152 mg·g^{-1}) have poor adsorption ability. Typically, poly(1,8-naphthylenediamine), poly(aniline-co-5-sulfo-2-anisidine) and PmPD-DEA***1.0*** have the relatively strongest Ag^+ adsorption ability (>2000 mg·g^{-1}). However, poly(1,8-naphthylenediamine) and poly(aniline-co-5-sulfo-2-anisidine) are difficult to use in industrial application due to the high cost of raw material.[37] Considering that, PmPD-DEA***1.0*** nanoparticles display a much better prospect in practical application.

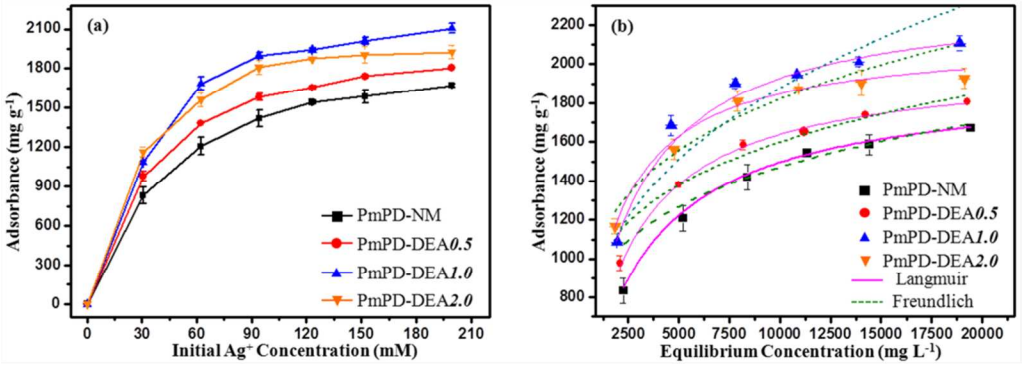

Fig. 7 Ag^+ adsorption with different initial Ag^+ concentrations between 0-200 mM.

Table 2 Parameters of Langmuir and Freundlich models simulated by no-liner fit for the adsorption of Ag^+ on PmPD.

PmPD-name	Langmuir model			Freundlich model		
	K_L	Q_m (mg·g^{-1})	R^2	K_F	1/n	R^2
NM	0.0379	1920.766	0.995	562.997	0.212	0.871
DEA***0.5***	0.0474	2016.868	0.996	610.105	0.213	0.956
DEA***1.0***	0.0480	2359.276	0.995	454.850	0.313	0.957
DEA***2.0***	0.0701	2132.469	0.992	655.886	0.226	0.918

Competitive adsorption. The effect of coexisting ions (Pb^{2+}, Zn^{2+}, Cu^{2+}) on Ag^+ adsorption was examined. PmPD-DEA***1.0*** was used here considering its better performance. Since the adsorbance of PmPD-DEA***1.0*** is high, there still leaves abundant adsorption sites after treating one kind of metal ion in low concentration. Therefore, a relatively high concentration (10 mM) of these four ions was selected to evaluate the competiveness of Ag^+ during the adsorption. As seen in Table 3, although other ions exerting a gentle influence, the Ag^+ adsorbance of the sample still stays high. This proves that PmPD-DEA***1.0*** possesses a good selectivity for Ag^+.

Effect of adsorption time. Fig. 8(a) shows the Ag^+ adsorbance profile versus adsorption time on the products. Ag^+ adsorbance of PmPD-NM and PmPD-DEA***1.0*** increases nonlinearly with adsorption time. The adsorption process can be roughly divided into fast and slow stages. The fast adsorption may be attributed to the physical surface adsorption of Ag^+ on the high surface energy particles.[38] By further extending the reaction time, the adsorbance increases slowly. This may result from redox and chelation reactions between Ag^+ and functional groups of the product. The adsorption process tends to be equilibrium when the adsorption time lasts as long as ~72 h.

To investigate the mechanism of adsorption, nonlinear first- and second-order kinetic models are applied and presented in Fig. 8(b). The kinetic parameters and the R^2 are given in Table 4. From it we can conclude that the second-order equation can better fit for the adsorption process since its correction efficiency is higher than the fist-order equation. That means the adsorption tends to be a chemical process through valency force between PmPD and Ag^+ ions.[37]

Table 3 Selective adsorption of PmPD-DEA***1.0***.[a]

Initial ion concentration (mM)				Ion adsorbance (mg·g^{-1})			
Ag^+	Pb^{2+}	Zn^{2+}	Cu^{2+}	Ag^+	Pb^{2+}	Zn^{2+}	Cu^{2+}
10	/	/	/	623.9±46.1	/	/	/
10	10	10	10	539.3±57.7	109.4±27.9	45.1±7.3	25.7±6.4

[a] Adsorption conditions: 20 mL solution, 25 mg PmPD-DEA***1.0***, 24 h, 30°C.

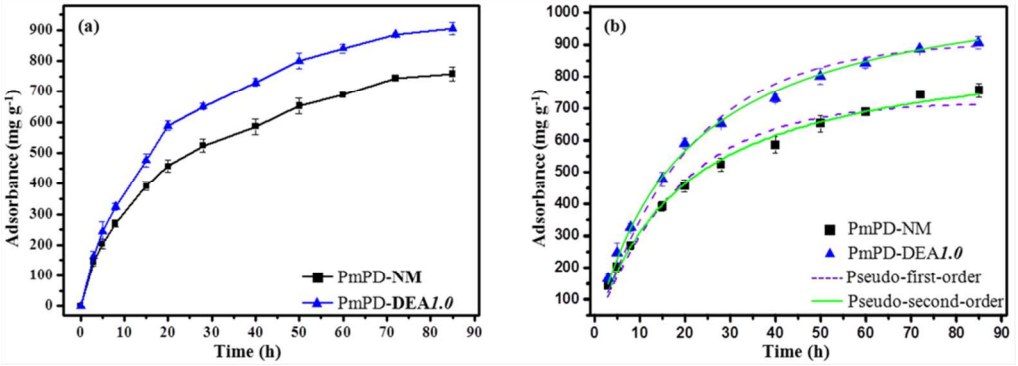

Fig. 8 Ag^+ adsorption with different adsorption time between 0-82 h. Initial concentration of Ag^+ is 15 mM.

Table 4 Kinetic parameters of Pseudo-first and –second models simulated by no-liner fit for the adsorption of Ag^+ on PmPD.

PmPD-name	$Q_{e,exp}$ (mg·g^{-1})	Pseudo-first-order model			Pseudo-second-order model		
		k (min^{-1})	$Q_{e,cal}$ (mg·g^{-1})	R^2	h (min^{-1})	$Q_{e,cal}$ (mg·g^{-1})	R^2
NM	758.1±22.0	0.05389	720.126	0.9881	0.00005680	912.597	0.9965
DEA***1.0***	905.2±19.5	0.04783	910.303	0.9896	0.00004446	1128.121	0.9980

Generally, Ag^+ is adsorbed on the deprotonated polymers that have certain reducibility by three adsorption process: physical adsorption, chelation adsorption and redox adsorption.[5] Since the PmPD has a relatively high surface energy, surface physical adsorption must occur through weak van der Waals force between Ag^+ and adsorbent although this interaction is not stable. The chelation adsorption mainly takes place between neutral amine/imine groups and Ag^+ in the initial stage of adsorption,[39, 40] depicted in Scheme S1A. More importantly, with increasing adsorption time, redox adsorption is believed to be the predominant mechanism,[38] during which Ag^+ ions act as oxidant and PmPD particles as a reductant. Ag^+ ions are reduced to Ag^0 metal, as evidenced by the TEM image, FTIR spectra and XRD patterns of PmPD-DEA***1.0*** before and after adsorbing Ag^+ (Fig. S4, S5 and S6). Meanwhile, benzenoid amine of the polymer are oxidized to quinoid imine (Scheme S1B), which possibly further returns to benzenoid amine through hydrolysis catalyzed by H^+ protonation to again reduce the Ag^+ ions. These "oxidation-reduction cycles" have been reported by others[41,42] and we believe its existence in our research.

Conclusions

In this study, we reported the high-yield synthesis of PmPD hollow nanostructures with enhanced surface area and low oxidation state through introducing DEA into the reaction system by conventional chemical oxidative polymerization. DEA concentration of ~1.0 M is optimal to the formation of nano-sized hollow structures of PmPD. The obtained product with high surface area shows superior adsorbability towards Ag^+ with the maximum adsorbance of 2359.3 mg·g^{-1} and has a good selectivity for Ag^+. The adsorption behaviour can be described by Langmuir and pseudo-second-order models. Moreover, this DEA-assisted method is facile and low cost and may be hopefully applied to prepare other aromatic diamine polymer with interesting morphology.

Acknowledgements

This research was supported by the program for Changjiang Schalors, National Funds for Distinguished Young Scientists of China (2011AA0610011), the National Natural Science Foundation of China (Grant 51374237), the Award for Excellent Doctoral Student Granted by Ministry of Education, China (113501027), Shanghai Tongji Gao Ting-Yao Environmental Science and Technology Development Foundation.

Notes and References

[a] *Department of Environmental Engineering, School of Metallurgical Science and Engineering, Central South University, Changsha 410017, China. Fax: +86-0731-88710171; Tel: +86-0731-88836804; E-mail: haiyw25@yahoo.com*

[b] *National Engineering Research Center for Heavy Metals Pollution Control and Treatment, Changsha 410017, China. Fax: +86-0731-88710171; Tel: +86-0731-88836804; E-mail: haiyw25@yahoo.com*

[c] *Zhen Su and Liyuan Zhang share the first author.*

* *Corresponding author: Fax: +86-0731-88710171; Tel: +86-0731-88836804; E-mail: haiyw25@yahoo.com*

† Electronic Supplementary Information (ESI) available: Fig. S1: X-ray diffractograms of PmPD; Fig. S2 TG of PmPD prepared with or without the aid of DEA; Fig. S3 TEM image of PmPD synthesized with the aid of DPA; Fig. S4 TEM image of PmPD-DEA1.0 after adsorbing AgNO3 solution; Fig. S5 FTIR of PmPD-DEA1.0 after adsorbing AgNO3 solution; Fig. S6 XRD of the PmPD-DEA1.0 after Ag^+ adsorption; Table S1 Comparison of the Ag^+ adsorbance of other common adsorbents; Scheme S1. Reaction of benzenoid amine and quinoid imine with Ag^+. See DOI: 10.1039/b000000x/

1. X. G. Li, X. L. Ma and M. R. Huang, *Chin. J. Anal. Chem.*, 2008, **36**, 253.
2. J. Tian, Y. Luo, H. Li, W. Lu, G. Chang, X. Qin and X. Sun, *Catal. Sci. Technol.*, 2011, **1**, 1393.
3. M. R. Huang, X. W. Rao, X. G. Li and Y. B. Ding, *Talanta*, 2011, **85**, 1575.
4. M. R. Huang, Y. B. Ding and X. G. Li, *Analyst*, 2013, **138**, 3820.
5. L. Y. Zhang, L. Y. Chai, J. Liu, H. Y. Wang, W. T. Yu and P. L. Sang, *Langmuir*, 2011, **27**, 13729.
6. W. T. Yu, L. Y. Zhang, H. Y. Wang and L. Y. Chai, *J. Hazard. Mater.*, 2013, **260**, 789.

7. Z. Su, L. Y. Zhang, L. Y. Chai, W. T. Yu, H. Y. Wang and Y. Shi, *Rsc Adv.*, 2013, **3**, 8660.
8. P. L. Sang, Y. Y. Wang, L. Y. Zhang, L. Y. Chai and H. Y. Wang, *Trans. Nonferrous Met. Soc. China*, 2013, **23**, 243.
9. M. R. Huang, Q. Y. Peng and X. G. Li, *Chem. Eur. J.*, 2006, **12**, 4341.
10. R. Tang, Q. Li, L. Ding, H. Cui and J. Zhai, *Environ. Technol.*, 2012, **33**, 341.
11. A. Xie, L. Ji, S. Luo, Z. Wang, Y. Xu and Y. Kong, *New J. Chem.*, 2014, **38**, 777.
12. Q. F. Lü, M. R. Huang and X. G. Li, *Chem. Eur. J.*, 2007, **13**, 6009.
13. M. R. Huang, H. J. Lu, W. D. Song and X. G. Li, *Soft Materials*, 2010, **8**, 149.
14. L. Zhang, T. Lin, X. Pan, W. Wang and T.-X. Liu, *J. Mater. Chem.*, 2012, **22**, 9861.
15. W. Fan, C. Zhang, W. W. Tjiu, K. P. Pramoda, C. He and T. Liu, *ACS Appl. Mat. Interfaces*, 2013, **5**, 3382.
16. J. Han, J. Dai and R. Guo, *J. Colloid Interface Sci.*, 2011, **356**, 749.
17. J. M. D'Arcy, H. D. Tran, A. Z. Stieg, J. K. Gimzewski and R. B. Kaner, *Nanoscale*, 2012, **4**, 3075.
18. J. Han, P. Fang, J. Dai and R. Guo, *Langmuir*, 2012, **28**, 6468.
19. W. Z. Niu, Z. Z. Yang, Z. B. Hu, Y. F. Lu and C. C. Han, *Adv. Funct. Mater.*, 2003, **13**, 949.
20. J. Han, G. Song and R. Guo, *Eur. Polym. J.*, 2007, **43**, 4229.
21. S. Yang, D. Liu, F. Liao, T. Guo, Z. Wu and T. Zhang, *Synth. Met.*, 2012, **162**, 2329.
22. T. T. Guo, F. Liao, Z. F. Wang and S. W. Yang, *J. Mater. Sci. Res.*, 2012, **1**, 25.
23. L. Y. Zhang, H. Y. Wang, W. T. Yu, Z. Su, L. Y. Chai, J. H. Li and Y. Shi, *J. Mater. Chem.*, 2012, **22**, 18244.
24. D. Ichinohe, K. Akagi and H. Kise, *Synth. Met.*, 1997, **85**, 1671.
25. X. G. Li, W. Duan, M. R. Huang and Y. L. Yang, *J. Polym. Sci., Part A: Polym. Chem.*, 2001, **39**, 3989.
26. X. G. Li, M. R. Huang and Y. Yang, *polymer*, 2001, **42**, 4099.
27. X. G. Li, M. R. Huang, W. Duan and Y. L. Yang, *Chem. Rev.*, 2002, **102**, 2925.
28. M. R. Huang, H. J. Lu and X. G. Li, *J. Mater. Chem.*, 2012, **22**, 17685.
29. X. G. Li, W. Duan, M. R. Huang, Y. L. Yang, D. Y. Zhao and Q. Z. Dong, *Polymer*, 2003, **44**, 5579.
30. M. Trchova, I. Sedenkova, E. N. Konyushenko, J. Stejskal, P. Holler and G. Ciric-Marjanovic, *J. Phys. Chem. B*, 2006, **110**, 9461.
31. B. J. Kim, S. G. Oh, M. G. Han and S. S. Im, *Langmuir*, 2000, **16**, 5841.
32. I. Sapurina and J. Stejskal, *Polym. Int.*, 2008, **57**, 1295.
33. M. X. Wan, *Adv. Mater.*, 2008, **20**, 2926.
34. Z. Zhang, Z. Wei and M. Wan, *Macromolecules* 2002, **35**, 5937.
35. H. D. Tran, Y. Wang, J. M. D'Arcy and R. B. Kaner, *Acs Nano*, 2008, **2**, 1841.
36. J. J. Wang, J. Jiang, B. Hu and S. H. Yu, *Adv. Funct. Mater.*, 2008, **18**, 1105.
37. X. G. Li, X. L. Ma, J. Sun and M. R. Huang, *Langmuir*, 2009, **25**, 1675.
38. X. G. Li, H. Feng and M. R. Huang, *Chem. Eur. J.*, 2010, **16**, 10113
39. C. M. S. Izumi, H. F. Brito, A. M. D. C. Ferreira, V. R. L. Constantino and M. L. A. Temperini, *Synth. Met.*, 2009, **159**, 377.
40. M. R. Huang, S. J. Huang and X. G. Li, *J. Phys. Chem. C*, 2011, **115**, 5301.
41. E. T. Kang, K. G. Neoh and S. W. Huang, *J. Phys. Chem. B*, 1997, **101**, 10744.
42. J. Stejskal, M. Trchová, J. Kovářová, J. Prokeš and M. Omastová, *Chemical Papers*, 2008, **62**, 181.